Whispering Gallery Modes and Frequency Combs: Two excursions in the world of photonic resonators

Monique Dauge, Stéphane Balac, Gabriel Caloz, Zoïs Moitier

Whispering Gallery Modes and Frequency Combs: Two excursions in the world of photonic resonators

Monique Dauge[1,*], **Stéphane Balac**[1], **Gabriel Caloz**[1], **Zoïs Moitier**[2]

[1]IRMAR, Université de Rennes, France
[2]ENSTA Paris, France

[*]Email: monique.dauge@univ-rennes1.fr

Abstract

In photonics, resonators are versatile elements designed with the aim of guiding light. They encompass various orders of magnitude for their sizes and the power of their laser sources. Accordingly some effects can be considered as negligible, leading to simplified mathematical models. We will focus on two such models: one related to Whispering Gallery Mode resonators and the other to ring/Fabry-Perot resonators.

In the first case the retained model leads to a two-dimensional linear Helmholtz equation in the whole space with material laws having a jump along a bounded interface. The set of complex resonances is analyzed close to the real axis, corresponding to modes concentrated close to the interface.

In the second case a one-dimensional model with cubic nonlinearity based on the Lugiato-Lefever equation is considered. Branches of stationary solutions issued from flat solutions are highlighted, providing frequency comb solutions.

Keywords: Whispering gallery mode, Frequency comb, Scattering resonances, Lugiato-Lefever equation

1 Physical motivations

Whispering gallery mode (WGM) resonators are miniaturized dielectric or metallic optical devices at micro- or nano-scale that have become invaluable in integrated photonics. The response of such resonators is mainly driven by the behavior of their complex resonances (1), in particular close to the real axis where they partly share some properties of conservative systems, see [8] where the notion of quasi-normal mode is introduced and discussed. Such resonances can form combs or lattices.

An other kind of optical resonator generating frequency combs are ring or Fabry-Perot (FP) resonators [4]. They are formed by an optical fiber either closed or bounded at each end by a multi-layer dielectric mirror. Their operation relies on third order polarization nonlinearities. Their ease of design combined with their compactness make them an interesting alternative to WGM resonators [12]. Ring and FP resonators are classically modelized by a Lugiato-Lefever equation (LLE), see (11), the stationary solutions of which may display frequency combs.

The modal study of WGM resonators presented in Section 2 has its root in a collaboration of the authors with FOTON Institute (`http://foton.cnrs.fr`) whereas the investigation of ring/FP resonators presented in Section 3 is part of the ANR project Rollmops led by LAAS laboratory (`https://www.laas.fr`).

2 Whispering gallery vs plasmonic modes

A bounded domain $\mathsf{C} \subset \mathbb{R}^2$ with smooth boundary is given, accounting for the cavity of the resonator. The relative electric permittivity ε is defined on the whole $\mathbb{R}^2$ and satisfies

$$\varepsilon(x) = 1, \ \ \forall x \notin \mathsf{C} \quad \text{and} \quad \varepsilon(x) = \varepsilon_{\mathsf{c}}(x), \ \forall x \in \mathsf{C}$$

where the function ε_{c} describes the properties of the cavity. We address the following two cases:

(i) $\varepsilon_{\mathsf{c}} = n_{\mathsf{c}}^2(r)$ with the optical index $n_{\mathsf{c}} > 1$ on $\overline{\mathsf{C}}$ (case of dielectric micro-resonator).

(ii) ε_{c} is a negative constant (case of metallic nano-resonators).

Our aim is to find modes u that are locally in H^1 and complex frequencies k such that

$$\begin{cases} -\operatorname{div}\left(\dfrac{1}{\varepsilon}\nabla u\right) - k^2\, u = 0 & \text{in } \mathbb{R}^2 \qquad (1a) \\ \text{outgoing radiation cond.} & |x| \to +\infty \qquad (1b) \end{cases}$$

with special emphasis on modes u concentrated along the interface $\partial\mathsf{C}$ and frequencies k close to the real axis (thus corresponding to large quality factors). The Helmholtz equation (1a) is not a classical eigenvalue problem for a self-adjoint operator with compact resolvent, but

rather belongs to the category of scattering resonance problems for which a radiation condition (1b) has to be associated. At a more general level, the transmission operator P defined as $-\operatorname{div}\left(\frac{1}{\varepsilon}\nabla u\right)$ can be viewed as a *black box Hamiltonian* in the sense of [6, §4.1] because the support of the function $\varepsilon - 1$ is compact. At this level, scattering resonances are defined as $k = \sqrt[+]{z}$ where the complex numbers z are the poles of the extended resolvent $(P-z)^{-1}$, obtained by extension from the complex upper plane $\mathbb{C}^+$ to the complex lower plane $\mathbb{C}^-$. More practically, radiation condition (1b) can be read on the asymptotics at infinity of solutions u of equation (1a): For $|x|$ large enough, such u can be expanded in polar coordinates (r,θ) using Hankel functions of first and second kind

$$u = \sum_{m\in\mathbb{Z}} \left(a_m \mathrm{H}_m^{(1)}(kr) + b_m \mathrm{H}_m^{(2)}(kr)\right) e^{\mathrm{i}m\theta}. \quad (2)$$

Since $\mathrm{H}_m^{(1)}$ and $\mathrm{H}_m^{(2)}$ are exponentially decreasing and increasing, respectively, in $\mathbb{C}^+$, condition (1b) consists in stating that $b_m = 0$ for any m.

Resorting to blackbox Hamiltonians where the technique of [13] is valid, we recast problem (1) in a family of *semiclassical* problems in which the small parameter h can be viewed as the inverse of the angular frequency m present in (2). This can be clearly seen if the cavity C is a disc (with center 0 and radius R) and the function ε is radial. Then the coefficients u_m in the expansion $\sum_{m\in\mathbb{Z}} u_m(r)\, e^{\mathrm{i}m\theta}$ of u in polar coordinates satisfy the equation

$$-\frac{1}{r}\partial_r\left(\frac{r}{\varepsilon}\partial_r u_m\right) + \frac{m^2}{\varepsilon\, r^2}\, u_m = k^2\, u_m \quad (3)$$

Setting $h = \frac{1}{m}$, $\mathcal{H} = \frac{1}{r}\partial_r(\frac{r}{\varepsilon}\partial_r)$, $E_h = \frac{k^2}{m^2}$, and

$$V(r) = \frac{1}{\varepsilon(r)\, r^2} \quad (4)$$

we find that (3) writes in the form of a Schrödinger equation with potential V:

$$-h^2\,\mathcal{H}w_h + V w_h = E_h w_h\,. \quad (5)$$

2.1 Dielectric case *(i)*

When ε_{c} is a constant > 1, we see that V has always a local minimum at the cavity boundary $r = R$ (configuration $\boxed{\text{A}}$, see Fig. 1 left). In the more general case of a *graded index* n_{c}, the properties of V mainly depend on the limits as $r \nearrow R$ of n_{c} and of its first and second derivatives (denoted by n_0, n_1, and n_2). Introduce in particular the *effective curvature*

$$\breve{\kappa} = 1 + R\frac{n_1}{n_0}\,, \quad (6)$$

and define configuration $\boxed{\text{B}}$ by the condition $\breve{\kappa} = 0$, see Fig. 1 right.

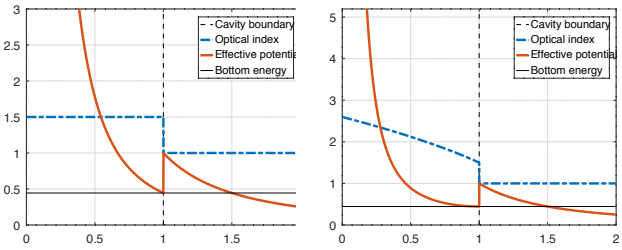

Figure 1: V for constant or graded indices with $n_{\mathsf{c}} = n_0$ for $\boxed{\text{A}}$ and $n_{\mathsf{c}}(r) = n_0\sqrt{1+2(1-r)}$ for $\boxed{\text{B}}$ (here $R = 1$, $n_0 = 1.5$).

Our analysis relies on the construction of *quasimodes* $(\underline{k}(m), \underline{u}(m))$ at any order as $m \to \infty$, i.e. approximate solutions of (3) with residuals m^{-N} for any $N \in \mathbb{N}$. The discontinuity of the derivative of V at the bottom of its well in $r = R$ implies that $\underline{u}$ has two different boundary layer scales as $r \nearrow R$ and $r \searrow R$. Here follows application of results [1, 2] in the case of a disc cavity in configurations $\boxed{\text{A}}$ and $\boxed{\text{B}}$

Theorem 1 *For any integer $j \geq 1$, there exists a quasimode $\left(\underline{k}_j(m), \underline{u}_j(m)\right)$ of the form:*

Configuration $\boxed{\text{A}}$. *$\underline{k}_j(m)$ has an expansion in integer powers of $m^{-1/3}$ starting as*

$$\frac{m}{Rn_0}\left[1 + \frac{a_j}{2}\left(\frac{2}{m}\right)^{\frac{2}{3}} - \frac{1}{2n_0 n_0'}\left(\frac{2}{m}\right) + \mathcal{O}(m^{-\frac{4}{3}})\right] \quad (7)$$

in which $0 < a_1 < a_2 < \dots$ are the zeros of the reverse Airy function and $n_0' = \sqrt{n_0^2 - 1}$.

Configuration $\boxed{\text{B}}$. *$\underline{k}_j(m)$ has an expansion in integer powers of $m^{-1/2}$ starting as*

$$\frac{m}{Rn_0}\left[1 + \frac{(4j-1)\sqrt{\mu}}{2}\left(\frac{1}{m}\right) + \mathcal{O}(m^{-\frac{3}{2}})\right] \quad (8)$$

in which $\mu = 2 - R^2 n_2/n_0$.

Moreover [2] proves that the quasi-resonances $\underline{k}_j(m)$ are close to true resonances $k_j(m)$ modulo a super-algebraic error $\mathcal{O}(m^{-\infty})$ by showing that the result of [13] applies to these cases.

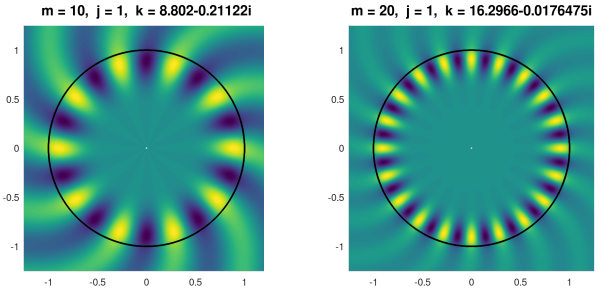

Figure 2: Real part for modes $j = 1$ for $m = 10$ (left) and $m = 20$ (right) in configuration A.

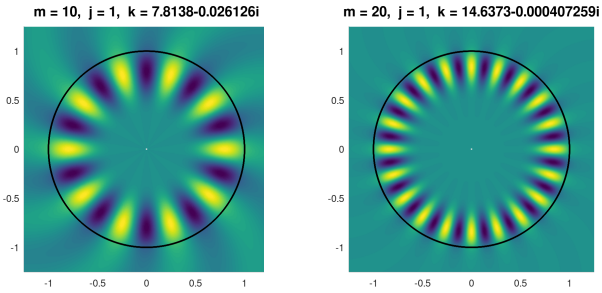

Figure 3: Real part for modes $j = 1$ for $m = 10$ (left) and $m = 20$ (right) in configuration B.

Numerical experiments using Perfectly Matched Layers suggest that the eigenvectors $u_j(m)$ themselves have the structure predicted by the quasi-eigenvectors $\underline{u}_j(m)$ with an angular frequency m and boundary layers of each side of the boundary $\partial\mathsf{C}$ of the cavity with asymptotic profiles at predicted scales, see Fig. 2 and 3. Such concentration of eigenvectors around $\partial\mathsf{C}$ justify the denomination *whispering gallery mode*.

The radiating field outside the cavity ($r > R$) decreases as $e^{-m(r-R)}$ inside a large layer around C. For $r < R$, the modes concentrate near $r = R$ with the scale $m^{2/3}(R - r)$ in configuration A, and with the scale $m^{1/2}(R - r)$ in configuration B.

2.2 Sign-changing case *(ii)*

When ε_{c} is a negative constant, the structure of the Schrödinger equation (5) is non standard since $\mathcal{H}$ contains a change of sign. Nevertheless, when $\varepsilon_{\mathsf{c}} < -1$, *one family* of quasimodes $\big(\underline{k}(m), \underline{u}(m)\big)$ can be constructed [3] in a similar spirit as in case *(i)*, yielding quasi-resonances $\underline{k}(m)$ with an expansion in integer powers of m^{-1} starting as

$$\frac{m}{R\eta_0}\sqrt{\eta_0^2 - 1}\Big[1 + \frac{1-\eta_0^2}{2\eta_0}\Big(\frac{1}{m}\Big) + \mathcal{O}(m^{-2})\Big] \quad (9)$$

in which $\eta_0^2 = -\varepsilon_{\mathsf{c}}$.

The application of [13] to obtain that quasi-resonances $\underline{k}(m)$ are close to true resonances $k(m)$ modulo $\mathcal{O}(m^{-\infty})$ is still possible, though more delicate [9]. Again, numerical experiments using PML exhibit results very close to asymptotic structures. In particular, eigenvectors are more concentrated around the boundary $\partial\mathsf{C}$, namely at scale $m(R - r)$, just like outside C, Fig. 4. Now such structure is referred at by the term *plasmonic modes*.

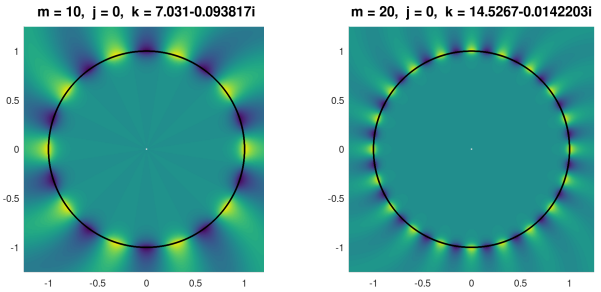

Figure 4: Real part for modes for $m = 10$ (left) and $m = 20$ (right) for $\varepsilon_{\mathsf{c}} = -2.25$.

2.3 Contrasting features

In both cases *(i)* and *(ii)* the asymptotic formulas account for a small though infinite set of resonances among a much wider set. In case *(i)*, none of them correspond to an eigenvalue, in contrast with case *(ii)* for which there exists an infinite sequence of *negative eigenvalues* z_n corresponding to pure imaginary eigenfrequencies $k_n = \mathrm{i}\sqrt{-z_n}$. When $\varepsilon_{\mathsf{c}} < -1$ they have a semiclassical structure and can be organized in WGM families like (7). When $\varepsilon_{\mathsf{c}} \in (-1, 0)$, we find no resonance close to the real axis, but one more family of eigenvalues with a structure reminding (9).

The configuration of non circular cavities C can be handled by a more delicate technique using expansions in tubular coordinates around $\partial\mathsf{C}$ and a WKB ansatz in the curvilinear abscissa along $\partial\mathsf{C}$. The construction shows that *positive effective curvature* is necessary to generate WG modes in case *(i)* whereas the change of sign is sufficient to generate plasmonic modes in case *(ii)*, see the peanut example in [3, Fig. 10, left].

2.4 Imaginary part of resonances

The constructed quasi-resonances $\underline{k}_j(m)$ are real and positive, tending to infinity with m. Since they are close to true resonances $k_j(m)$ modulo $m^{-\infty}$, this in particular implies that the cor-

responding true resonances have a very small imaginary part. By analogy with the results of [7] obtained for *analytic potentials*, we find it plausible to observe an *exponential decay* of the imaginary parts of the resonances $k_j(m)$, conjecturing asymptotics like

$$\operatorname{Im} k_j(m) \sim e^{-2S_0 m}, \quad j \geq 1 \tag{10}$$

with S_0 given by $\int_R^{\lambda_0^{-1/2}} \sqrt{V(r)-\lambda_0}\,\mathrm{d}r$ where λ_0 is the bottom energy $1/(n_0^2R^2)$. In order to check such a behavior through numerical experiments, we used a quadruple precision `Julia` program coding a finite difference method with a 6-stage extrapolation to get an enhanced precision, allowing to reach imaginary parts as small as 10^{-30} instead of 10^{-12} with usual double precision arithmetics, see Fig. 5 for configuration A with $\varepsilon_c = 2.25$ and $j = 1, 2, 3$.

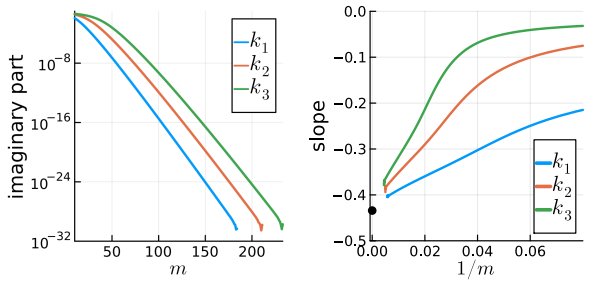

Figure 5: Left, $\operatorname{Im} k_j(m)$ vs m. Right, the slope $\log\left|\operatorname{Im} k_j(m+1)\right| - \log\left|\operatorname{Im} k_j(m)\right|$ vs $1/m$, expected to converge to $-2S_0$ (marked with •), *cf* (10).

3 Frequency combs

After reduction and nondimensionalization, frequency combs can be closely related to *complex solutions* $\psi = \psi(\theta, t)$ of some Lugiato Lefever Equations. Here t is the time and θ is the one-dimensional periodic space variable in the torus $\mathbb{T} = \mathbb{R}/(2\pi\mathbb{Z})$. Depending on the *real parameters* d (dispersion), α (detuning), f (driving force), and σ (switch between ring and FP resonator) the evolution equation writes

$$\partial_t\psi = \mathrm{i}d\,\partial_\theta^2\psi - (1+\mathrm{i}\alpha)\psi + \mathrm{i}\psi\Big(|\psi|^2 + \frac{\sigma}{\pi}\int_{\mathbb{T}} |\psi(\vartheta,\cdot)|^2\,\mathrm{d}\vartheta\Big) + f. \tag{11}$$

More specifically, f is a positive constant, σ is set to 0 for ring resonators and to 1 for FP resonators. Even when $\sigma = 0$, the presence of the detuning parameter α is a distinctive feature when compared to the nonlinear cubic Schrödinger equation, causing the loss of Hamiltonian structure.

Here we focus on stationary solutions $\psi = \psi(\theta)$ and present for the case $\sigma = 0$ a method using common features to both cases $\sigma = 0$ or 1, making possible the adaptation to the case $\sigma = 1$ by mere calculation.

Constant stationary solutions of (11) are well known: They are complex numbers a satisfying

$$-(1+\mathrm{i}\alpha)\,a + \mathrm{i}a|a|^2 + f = 0. \tag{12}$$

Depending on f and α, there exist between 1 and 3 such *flat solutions*. In order to have a global parametrization, it is valuable to introduce the parameter ρ accounting for the squared modulus $|a|^2$ of a flat solution.

Lemma 2 *Let $\alpha \in \mathbb{R}$ be chosen. For any $\rho > 0$, there exists a unique positive number $f = f(\rho)$ and a unique complex number $a = a_(\rho)$ such that $|a|^2 = \rho$ and (12) holds.*

Although the flat solutions are not the solutions that are relevant from the physical point of view, they are of utmost importance because they can be onsets of bifurcation branches among stationary solutions of (11).

Following the idea of [10], we resort to the theory of Crandall and Rabinowitz [5]:

Theorem 3 *An equation of type $\mathcal{F}(u,\lambda) = 0$ in which u belongs to a Hilbert space and λ to an interval, and such that $u = 0$ is solution for all λ, possesses one (and only one) branch of non-trivial solutions starting from $(0,\lambda_0)$ if conditions $(\mathcal{H}0)$-$(\mathcal{H}2)$ are satisfied:*

- $(\mathcal{H}0)$ **(Non-invertibility)** *The Fréchet derivative $(\partial_u\mathcal{F})_{(0,\lambda_0)}$ at point $(0,\lambda_0)$ is a non-invertible Fredholm operator with index 0.*
- $(\mathcal{H}1)$ **(Simplicity)** *The kernel of $(\partial_u\mathcal{F})_{(0,\lambda_0)}$ has dimension 1, let u_0 be a generator.*
- $(\mathcal{H}2)$ **(Transversality)** *The second derivative $(\partial_u\partial_\lambda\mathcal{F})_{(0,\lambda_0)}$ at point $(0,\lambda_0)$ applied to the kernel generator u_0 does not belong to the range of $(\partial_u\mathcal{F})_{(0,\lambda_0)}$.*

Moreover the branch of non-trivial solutions (u,λ) can be parametrized as (with $\eta > 0$)

$$u = \Phi(\tau), \quad \lambda = \mu(\tau), \quad \tau \in (-\eta,\eta) \tag{13}$$

with smooth functions Φ and μ if $\mathcal{F}$ is smooth.

Let α and d be chosen. Our problem can be written as

$$\mathcal{G}(\psi, f) = 0 \tag{14}$$

where

$$\mathcal{G}(\psi, f) = \mathrm{i}d\,\psi'' - (1+\mathrm{i}\alpha)\psi + \mathrm{i}\psi|\psi|^2 + f. \tag{15}$$

In order to use this theorem we have to recast our problem in the form $\mathcal{F}(u,\lambda) = 0$ in which $u = 0$ correspond to flat solutions and λ is a suitable parameter. For this we combine the global parametrization by ρ at fixed α (Lemma 2) with the idea in [11] of using a multiplicative perturbation formula, setting:

$$\mathcal{F}(u,\rho) := a(\rho)^{-1}\mathcal{G}\Big(a(\rho)(1+u),\, f(\rho)\Big). \tag{16}$$

For any flat solution a of the equation $\mathcal{G}(a,f) = 0$, we calculate the vector $B := (b_1, b_2)^\top$ where b_1 and b_2 are the real and imaginary parts of $a^{-1}\mathcal{G}\big(a(1+u), f\big)$, as a function of the vector $U = (u_1, u_2)^\top$ in which $u_1 + \mathrm{i}u_2 = u$. Like in [11], we find that B is the sum of a linear part $\mathcal{L}_\rho$, a quadratic part $\mathcal{L}_\rho^{(2)}$ and a cubic part $\mathcal{L}_\rho^{(3)}$ with quite simple structures:

$$\mathcal{L}_\rho = \begin{pmatrix} -1 & d\,\mathcal{D} + \alpha - \rho \\ -d\,\mathcal{D} - \alpha + 3\rho & -1 \end{pmatrix}$$

where $\mathcal{D}v = -v''$, and

$$\mathcal{L}_\rho^{(2)} = \rho\begin{pmatrix} -2u_1u_2 \\ 3u_1^2 + u_2^2 \end{pmatrix},\ \mathcal{L}_\rho^{(3)} = \rho\begin{pmatrix} -u_1^2u_2 - u_2^3 \\ u_1^3 + u_1u_2^2 \end{pmatrix}.$$

Note in particular that the flat solution a only appears through its squared norm ρ. Choose $\rho_0 > 0$. It is easy to see that

$$\partial_u\mathcal{F}_{(0,\rho_0)} = \mathcal{L}_{\rho_0},\quad \partial_u\partial_\rho\mathcal{F}_{(0,\rho_0)} = \begin{pmatrix} 0 & -1 \\ 3 & 0 \end{pmatrix}.$$

It is also easy to calculate $\mathcal{L}_{\rho_0}$ on the natural functional space of H^2-periodic functions on the torus $\mathbb{T}$ by Fourier expansion

$$U = \sum_{n\geq 0}\hat{U}_n^+\cos n\theta + \sum_{n\geq 1}\hat{U}_n^-\sin n\theta \tag{17}$$

where $\hat{U}_n^+$ and $\hat{U}_n^-$ are real 2-component vectors. As $\mathcal{D}\cos n\theta = n^2\cos n\theta$ and $\mathcal{D}\sin n\theta = n^2\sin n\theta$, we see that the Fourier expansion block diagonalizes $\mathcal{L}_{\rho_0}$ with the blocks ($n \in \mathbb{N}$)

$$\widehat{\mathcal{L}}_n = \begin{pmatrix} -1 & d\,n^2 + \alpha - \rho_0 \\ -d\,n^2 - \alpha + 3\rho_0 & -1 \end{pmatrix}.$$

At this stage, Th. 3 cannot be applied since condition ($\mathcal{H}1$) of simplicity is never satisfied (if $\widehat{\mathcal{L}}_k$ has a nonzero kernel, the dimension of $\ker\mathcal{L}_{\rho_0}$ is at least 2). As in [10], we choose to restrict to *synchronized* functions u, i.e. those satisfying $\hat{U}_n^- = 0$ for all n. In other words, the corresponding function space can be viewed as the domain of the Neumann realization of $\mathcal{D}$ on the half-interval $(0,\pi)$, for which an eigenvector basis is $\{\cos n\theta\}_{n\in\mathbb{N}}$. Synchronized solutions generate by symmetry and translations in space a whole bunch of periodic solutions, but it is still not known whether all periodic solutions are covered like this.

We find that ($\mathcal{H}0$) is satisfied at ρ_0 if there exists $k \in \mathbb{N}^*$ and $\varepsilon \in \{\pm 1\}$ with

$$dk^2 + \alpha = 2\rho_0 + \varepsilon\sqrt{\rho_0^2 - 1}\,, \tag{18}$$

that the transversality ($\mathcal{H}2$) holds if

$$\varepsilon = 1 \quad \text{or} \quad \rho_0 \neq \frac{2}{\sqrt{3}} \quad (\simeq 1.155). \tag{19}$$

Let us choose $\rho_0 \geq 1$, $k \in \mathbb{N}^*$ and $\varepsilon \in \{\pm 1\}$ so that (18) and (19) hold. This leaves options for the application of Th. 3, namely the choice of the functional space $\mathcal{U}$ in which u is searched: $\mathcal{U}$ can be the space H^2 generated by $\cos n\theta$ functions for all $n \in \mathbb{N}$, but indeed, we can restrict n to integer multiples of k, and obtain a space $\mathcal{U}_k$ in which the stationary part of (11) still operates. The simplicity ($\mathcal{H}1$) in $\mathcal{U}_k$ requires that for all $N \in \mathbb{N}$, $dN^2k^2 + \alpha \neq 2\rho_0 - \varepsilon\sqrt{\rho_0^2 - 1}$.

Then, following (13), we can look for successive terms $\Phi^{(j)}$ and $\mu^{(j)}$ in the Taylor expansion at $\tau = 0$ of the nontrivial branch $(\Phi(\tau), \mu(\tau))$:

$$\begin{cases} u(\rho(\tau)) = \tau\Phi^{(1)} + \tau^2\Phi^{(2)} + \cdots \\ \rho(\tau) = \rho_0 + \tau\mu^{(1)} + \tau^2\mu^{(2)} + \cdots \end{cases} \tag{20}$$

This can be done by inserting these expansions into the equation $\mathcal{F}(u,\rho) = 0$. We obtain a sequence of equations, starting by $\mathcal{L}_{\rho_0}[\Phi^{(1)}] = 0$, and continuing by equations of the type

$$\mathcal{L}_{\rho_0}[\Phi^{(j)}] + \mu^{(j-1)}\partial_u\partial_\rho\mathcal{F}_{(0,\rho_0)}[\Phi^{(1)}] = f^{(j)}$$

where $f^{(j)}$ involves previous terms only. Remarkably, the transversality condition is the right one to ensure the solvability of these equations.

We can compute the first terms to get

$$\Phi^{(1)} = \begin{pmatrix} \rho_0 + \varepsilon\sqrt{\rho_0^2 - 1} \\ 1 \end{pmatrix}\cos k\theta,\quad \mu^{(1)} = 0,$$

and an explicit formula for $\mu^{(2)}$ as a function of $(\rho_0, \varepsilon, \alpha)$. The sign of $\mu^{(2)}$ determines whether the bifurcation is super- or sub-critical Fig. 6.

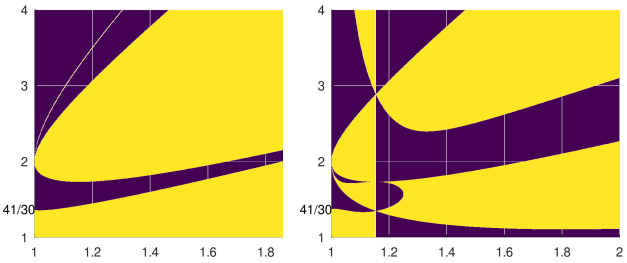

Figure 6: Sign of $\mu^{(2)}$ (+ (clear) or − (dark)) as function of $\rho \in [1,2]$, $\alpha \in [1,4]$, with $\varepsilon = 1$ left and $\varepsilon = -1$ right. Note the change of sign across the line $\rho = 2/\sqrt{3}$ where the transversality is not satisfied. The lowest change of sign on the axis $\rho = 1$ occurs at $\alpha = 41/30$

The value 1 is the least value of ρ_0 for which bifurcations may appear. When $\rho_0 = 1$, the coefficient $\mu^{(2)}$ depends only on α according to the formula

$$\mu^{(2)} = \frac{41 - 30\alpha}{9(2-\alpha)^2}$$

from which stems the famous value $\alpha = \frac{41}{30}$ where $\mu^{(2)}$ cancels when $\rho_0 = 1$, cf [11, sec. 3].

Using expansion (20), by setting

$$\psi(\rho) = a(\rho)(1 + u(\rho)) \quad \text{for} \quad \rho = \rho(\tau),$$

we can know the behavior of stationary solutions $(\psi(\rho), f(\rho))$ locally on the branch bifurcating from the trivial one at the point $(a(\rho_0), f(\rho_0))$.

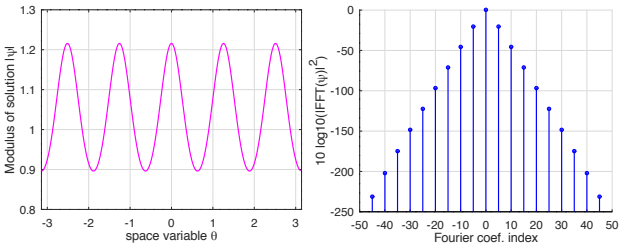

Figure 7: Norm (left) and Fourier coefficients (right) of solution at final time for $\alpha = 1$, $\rho_0 = 1.1$, $\varepsilon = 1$, $k = 5$, $(d = 0.06633)$, $\tau = 0.1$.

Due to unstable dynamics, computation by an evolution code of non-trivial branches near their onsets is difficult. We were nevertheless able to cross-check asymptotic expressions (20) with a split-step code in restricted regions of parameters, see Fig. 7 where the relative difference between computed solutions and formulas given by (20) is $\sim 0.4\%$. The frequency comb structure is visible on non-zero Fourier coefficients.

References

[1] S. Balac, M. Dauge, Y. Dumeige, P. Féron, and Z. Moitier, Mathematical analysis of whispering gallery modes in graded index optical micro-disk resonators, *Eur. Phys. J. D*, **74**:221 (2020).

[2] S. Balac, M. Dauge, and Z. Moitier, Asymptotics for 2D whispering gallery modes in optical micro-disks with radially varying index, *IMA Journal of Applied Mathematics*, **86**, 2 (2021), pp 1212-1265.

[3] C. Carvalho and Z. Moitier, Scattering resonances in unbounded transmission problems with sign-changing coefficient, *IMA Journal of Applied Mathematics*, **88**, 6 (2023), pp 1-43.

[4] Y. K. Chembo, Kerr optical frequency combs: theory, applications and perspectives, *Nanophotonics*, 5 (2016), pp. 214–230.

[5] M. G. Crandall and P. H. Rabinowitz, Bifurcation from simple eigenvalues, *J. Functional Analysis*, **8** (1971), pp 321-340.

[6] S. Dyatlov and M. Zworski, *Mathematical theory of scattering resonances*, Graduate Studies in Mathematics, **200** (2019).

[7] B. Helffer and J. Sjöstrand, *Résonances en limite semi-classique*, Mémoires de la Société Mathématique de France, **24-25** (1986).

[8] P. Lalanne, W. Yan, K. Vynck, C. Sauvan, and J. Hugonin, Light Interaction with Photonic and Plasmonic Resonances, *Laser & Photonics Reviews* **12**:1700113 (2018).

[9] R. Mandel, Z. Moitier, and B. Verfürth, Nonlinear Helmholtz equations with sign-changing diffusion coefficient, *Comptes Rendus. Mathématique* **360** (2022) pp 513-538

[10] R. Mandel and W. Reichel, A priori bounds and global bifurcation results for frequency combs modeled by the Lugiato-Lefever equation, *SIAM J. Appl. Math.*, **77** (2017), pp 315-345.

[11] T. Miyaji, I. Ohnishi, and Y. Tsutsumi, Bifurcation analysis to the Lugiato-Lefever equation in one space dimension, *Physica D: Nonlinear Phenomena*, **239** (2010), pp 2066-2083.

[12] J. Musgrave, S. Huang, and M. Nie, Microcombs in fiber Fabry–Perot cavities., *APL Photonics*, **8**:121101 (2023).

[13] S.-H. Tang and M. Zworski, From quasimodes to resonances, *Mathematical Research Letters*, **5** (1998), pp 261-272.